International Journal of Engineering

Comparison of MRAS Based Rotor Resistance Estimator Using Reactive Power and Flux Based Techniques for Space Vector PWM Inverter Fed Induction Motor Drives

M. Nandhini Gayathri [a *], S. Himavathi [b], R. Sankaran[a]

[a] Department of EEE, SASTRA University, Thanjavur -613 402, India
[b] Department of EEE, Pondicherry Engineering College, Puducherry - 605014, India

P A P E R   I N F O

A B S T R A C T

The performance of Vector Controlled Induction Motor drive depends on the accuracy of rotor resistance which will vary with temperature and frequency. The MRAS approach using reactive power and flux as a state variable for rotor resistance estimation makes MRAS computationally simpler and easy to design. In this paper, Rotor Flux based MRAS (RF-MRAS) and Reactive Power based MRAS (RP-MRAS) for rotor resistance estimation is designed and validated through MATLAB simulation. The performance of these two methods are analyzed extensively and compared in terms of accuracy and settling time. The suitable method for rotor resistance estimation for Space Vector PWM Inverter fed induction motor drive is identified. The promising obtained results are presented.

1. INTRODUCTION

Induction motors have several advantages compared to d.c motors: their low cost, robustness and reliability. Although, d.c machines have traditionally been used for high performance applications, the development of power electronics has contributed to the use of advanced control techniques that have made it possible to extend the use of induction machines in those applications [1, 2]. One of these techniques is the well known field oriented control. Traditionally, there have been two conventional methods which field oriented control is achieved by them: direct-field oriented control (DFOC) and indirect field oriented control (IFOC). Direct field oriented control requires explicit knowledge of the rotor field orientation. Indirect field oriented controller implements a closed-loop rotor flux controller and requires the angular position of the rotor flux which is calculated by integrating the angular speed [3]. This can be computed using the rotor speed and the stator current measurement. Unfortunately, the calculation of the angular position of the rotor flux is very sensitive to errors in rotor resistance which varies with the temperature. If care is not taken to compensate for the change, the flux orientation is lost, resulting in coupling between the *d*- and *q*-axes variables which leads to the

poor dynamic performance of the drive system [4-6]. Attention is focused for online estimation of rotor resistance for improved performance of field oriented control.

Various on-line rotor resistance estimation methods are proposed in the literature [7-21]. They are Least square sense Algorithm, spectral analysis techniques, Observer based techniques and Model Reference Adaptive System (MRAS). The MRAS scheme is popularly used for rotor resistance estimation because of its simpler implementation and less computational effort compared to other methods. MRAS observers are based on rotor flux and reactive power [5, 17]. In rotor flux based MRAS, the rotor flux error between reference and adjustable model is used by the adaptive mechanism for rotor resistance estimation. Whereas, in reactive power based MRAS, reactive power error is used instead of rotor flux error. The selection of reactive power as a state variable for MRAS based rotor resistance estimator results in a simpler system model which is easier to design. Both MRAS schemes have used PI controller as a part of the adaptive mechanism for rotor resistance estimation [10-12].

In this paper, two types of MRAS methods using flux, reactive power based technique for rotor resistance estimation is designed and validated through MATLAB simulation. The performance of these two methods are analyzed extensively and compared in terms of accuracy and settling time. The suitable method for rotor

---

[*]Corresponding Author Email: *nandhini.gayathri@gmail.com* (M. Nandhini Gayathri)

resistance estimation for Space Vector PWM Inverter fed induction motor drive is identified.

2. SCHEMATIC DIAGRAM OF SPACE VECTOR PWM INVERTER FED INDUCTION MOTOR DRIVE WITH ROTOR RESISTANCE ESTIMATOR

The vector control scheme presented here is indirect field oriented control (rotor flux oriented control). Figure 1 shows the overall block diagram of Space Vector PWM Inverter fed Induction Motor drive system with MRAS based rotor resistance estimator. The system consists of an Induction Motor drive system, rotor flux oriented control, Space Vector PWM Inverter along with flux and reactive power based MRAS rotor resistance estimator. Rotor flux oriented controller consists of a PI speed controller, a current controller, and a PWM generator.

3. SPACE VECTOR PWM INVERTER

The circuit model of a 6-pulse voltage source PWM inverter is shown in Figure 2. Phase voltage waveforms are shown in Figure 3 for 180° conduction mode. In Figure 2, S_1 to S_6 are the six power switches that shape the output, and are controlled by the logic variables a, a', b, b', c and c'. When an upper switch is switched on, i.e., when a, b (or) c is 1, the corresponding lower switch is

off, i.e., the corresponding a', b' (or) c' is 0. Therefore, the on and off states of the upper switches 1, 3 and 5 can be used to determine the output voltage waveforms [22, 23]. The relationship between the switching variable vector [a, b, c]^t and the line-to-line voltage vector [V_{ab}, V_{bc}, V_{ca}]^t is given by the following equation.

$$\begin{bmatrix} V_{ab} \\ V_{bc} \\ V_{ca} \end{bmatrix} = V_{dc} \begin{bmatrix} 1 & -1 & 0 \\ 0 & 1 & -1 \\ -1 & 0 & 1 \end{bmatrix} \begin{bmatrix} a \\ b \\ c \end{bmatrix} \tag{1}$$

Also, the relationship between the switching logic variable vector [a, b, c]^t and the phase voltage vector [V_{an}, V_{bn}, V_{cn}]^t can be expressed below.

$$\begin{bmatrix} V_{an} \\ V_{bn} \\ V_{cn} \end{bmatrix} = \frac{V_{dc}}{3} \begin{bmatrix} 2 & -1 & -1 \\ -1 & 2 & -1 \\ -1 & -1 & 2 \end{bmatrix} \begin{bmatrix} a \\ b \\ c \end{bmatrix} \tag{2}$$

Table 1 and Figure 4 shows the eight inverter voltage vectors (V_0 to V_7). From the table, the six non-zero space vectors are calculated in magnitude and space angle and are shown in Figure 4.
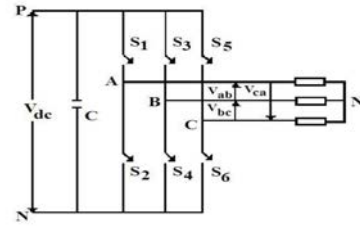

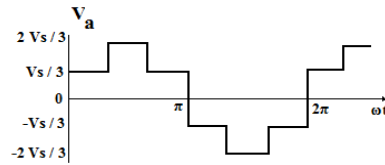**Figure 2.** Power circuit of a Three-phase Voltage source Inverter

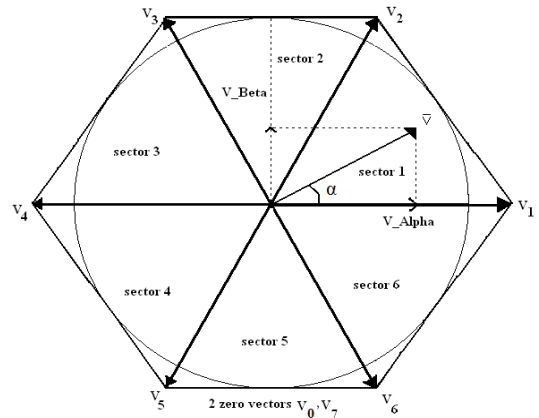**Figure 3.** Phase Voltage Waveform for 180 degree mode

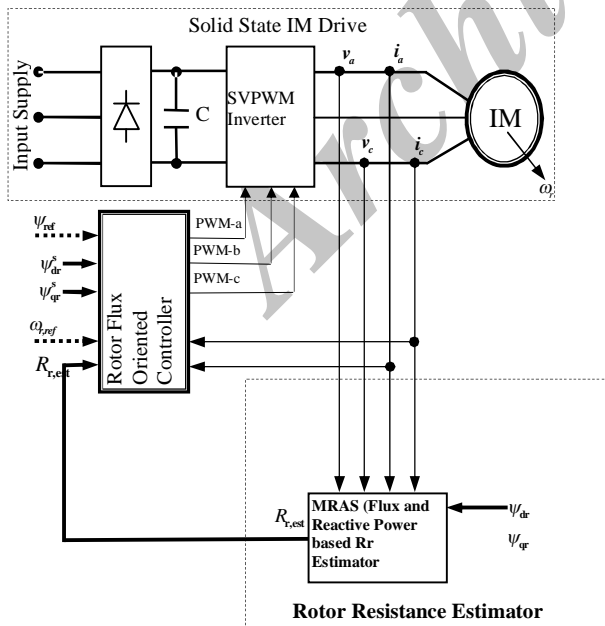**Figure 1.** Vector Controlled Induction Motor Drive showing Flux and Reactive Power based MRAS rotor resistance Estimator

Figure 4. Representation of Space Voltage Vector in Complex Plane

3. 1. Realization of Space Vector through PWM

In Space vector PWM inverter, six non-zero vectors and two zero vectors are presented [5]. Six nonzero vectors (V_1-V_6) shape the axes of a hexagon as depicted in Figure 4. The angle between any two adjacent non-zero vectors is 60 degrees. Meanwhile, two zero vectors (V_0 and V_7) are at the origin and apply zero voltage to the load. The eight vectors are called the primary space vectors and are denoted by V_0, V_1, V_2…V_7. The objective of SVPWM is to approximate the reference voltage vector V_{ref} using the eight switching patterns. One simple method of approximation is to generate the average output of the inverter in a small period to be the same as that of V_{ref} in the same period. T_z is the period of the high frequency modulating signal used for PWM of the inverter output. Referring to Figure 5, the space vector PWM is realized based on the following steps:

Step 1: Determine V_d, V_q, V_{ref} and angle α
Step 2: Determine time duration T_1, T_2, T_0

3. 1. 1. Step 1: Determine V_d, V_q, V_{ref} and Angle α

From Figure 5, the V_d, V_q, V_{ref} and angle α are functions of time and are determined in terms of the instantaneous phase voltages as follows:

$$V_d = V_{an} - V_{bn}.\cos 60 - V_{cn}.\cos 60 = V_{an} - \frac{1}{2}V_{bn} - \frac{1}{2}V_{cn}$$

$$V_q = 0 + V_{bn}.\cos 30 - V_{cn}.\cos 30 = V_{an} + \frac{\sqrt{3}}{2}V_{bn} - \frac{\sqrt{3}}{2}V_{cn} \tag{3}$$

$$\begin{bmatrix} V_d \\ V_q \end{bmatrix} = \frac{2}{3}\begin{bmatrix} 1 & -\frac{1}{2} & -\frac{1}{2} \\ 0 & \frac{\sqrt{3}}{2} & -\frac{\sqrt{3}}{2} \end{bmatrix}\begin{bmatrix} V_{an} \\ V_{bn} \\ V_{cn} \end{bmatrix} \tag{4}$$

$$\left| \overline{V}_{ref} \right| = \sqrt{V_d{}^2 + V_q{}^2}$$

$$\alpha = \tan^{-1}\left(\frac{V_q}{V_d}\right) = \omega t = 2\pi f t$$

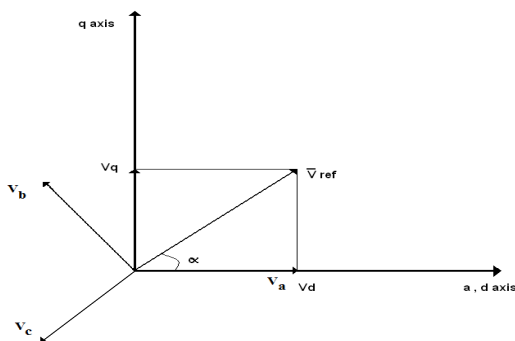where, f=fundamental frequency and assuming $\alpha = 0$ at t=0.

Figure 5. Components of Voltage Space Vector

3. 1. 2. Step 2: Determine Time Duration T_1, T_2, T_0

T_1, T_2, T_0 represent the time widths for vectors V_1, V_2, V_0, a is the modulation index and the super bar indicates average. By combining two successive switching periods T_z, there will be four null vectors per T_s, which is the sampling period.

3. 1. 3. Switching Time Duration at any Sector

With n representing sector number, (n=1,…6), the intervals T_1, T_2 and T_0 in any sector are derived as:

$$T_1 = \frac{\sqrt{3}.T_z.\left|\overline{V}_{ref}\right|}{V_{dc}}\left(\sin\left(\frac{\pi}{3} - \alpha + \frac{n-1}{3}\pi\right)\right)$$

$$= \frac{\sqrt{3}.T_z.\left|\overline{V}_{ref}\right|}{V_{dc}}\left(\sin\frac{n}{3}\pi\cos\alpha - \cos\frac{n}{3}\pi\sin\alpha\right) \tag{5}$$

$$T_2 = \frac{\sqrt{3}.T_z.\left|\overline{V}_{ref}\right|}{V_{dc}}\left(\sin\left(\alpha - \frac{n-1}{3}\pi\right)\right)$$

$$= \frac{\sqrt{3}.T_z.\left|\overline{V}_{ref}\right|}{V_{dc}}\left(-\cos\alpha.\sin\frac{n-1}{3}\pi + \sin\alpha.\cos\frac{n-1}{3}\pi\right) \tag{6}$$

$$T_0 = T_z - T_1 - T_2, \tag{7}$$

4. MRAS BASED ROTOR RESISTANCE ESTIMATION

The MRAS scheme consists of a reference model which determines the desired states and adaptive (adjustable) model which generates the estimated values of the states. The error between these states is fed to an adaptation mechanism to generate an estimated value of the rotor resistance which is used to adjust the adaptive model. This process continues till the error between two outputs tends to zero.

TABLE 1. Switching Time Calculation at Each Sector

Sector	Upper Switches (S_1, S_3, S_5)	Lower Switches (S_4, S_6, S_2)
1	$S_1 = T_1 + T_2 + T_0/2$	$S_4 = T_0/2$
	$S_3 = T_2 + T_0/2$	$S_6 = T_1 + T_0/2$
	$S_5 = T_0/2$	$S_2 = T_1 + T_2 + T_0/2$
2	$S_1 = T_1 + T_0/2$	$S_4 = T_2 + T_0/2$
	$S_3 = T_1 + T_2 + T_0/2$	$S_6 = T_0/2$
	$S_5 = T_0/2$	$S_2 = T_1 + T_2 + T_0/2$
3	$S_1 = T_0/2$	$S_4 = T_1 + T_2 + T_0/2$
	$S_3 = T_1 + T_2 + T_0/2$	$S_6 = T_0/2$
	$S_5 = T_2 + T_0/2$	$S_2 = T_1 + T_0/2$
4	$S_1 = T_0/2$	$S_4 = T_1 + T_2 + T_0/2$
	$S_3 = T_1 + T_0/2$	$S_6 = T_2 + T_0/2$
	$S_5 = T_1 + T_2 + T_0/2$	$S_2 = T_0/2$
5	$S_1 = T_2 + T_0/2$	$S_4 = T_1 + T_0/2$
	$S_3 = T_0/2$	$S_6 = T_1 + T_2 + T_0/2$
	$S_5 = T_1 + T_2 + T_0/2$	$S_2 = T_0/2$
6	$S_1 = T_1 + T_2 + T_0/2$	$S_4 = T_0/2$
	$S_3 = T_0/2$	$S_6 = T_1 + T_2 + T_0/2$
	$S_5 = T_1 + T_0/2$	$S_2 = T_2 + T_0/2$

Switching waveforms of S_1 to S_6 for all the sectors are obtained and are shown in Table 1.

4. 1. MRAS Based Rotor Resistance Estimation Using Rotor Flux

The block diagram of Rotor Flux-MRAS (RF-MRAS) is shown in Figure 6. In RF-MRAS, the used state variable is the rotor flux. The voltage model equations are used as the reference model because it is independent of rotor resistance. This model receives the machine stator voltages and current signals and calculates the rotor flux vector signals. The current model flux equations are used as an adaptive model because it is dependent on rotor resistance. This model can calculate fluxes from the input stator currents and speed only if the rotor resistance is known [5]. The equations defining the reference model and the adaptive model of induction machine are given in Equations (8) and (9) respectively.

The voltage model equations of the induction motor is given as

$$\begin{bmatrix} \dfrac{d\lambda dr}{dt} \\ \dfrac{d\lambda qr}{dt} \end{bmatrix} = \dfrac{Lr}{Lm} \left(\begin{bmatrix} vds \\ vqs \end{bmatrix} - \begin{bmatrix} Rs + s\sigma Ls & 0 \\ 0 & Rs + s\sigma Ls \end{bmatrix} \begin{bmatrix} ids \\ iqs \end{bmatrix} \right) \quad (8)$$

The current model equations of the induction motor is given as

$$\begin{bmatrix} \dfrac{d\lambda dr}{dt} \\ \dfrac{d\lambda qr}{dt} \end{bmatrix} = \begin{bmatrix} \dfrac{-1}{T_r} & -\omega_r \\ \omega_r & \dfrac{-1}{T_r} \end{bmatrix} \begin{bmatrix} \lambda dr \\ \lambda qr \end{bmatrix} + \dfrac{L_m}{T_r} \begin{bmatrix} ids \\ iqs \end{bmatrix} \quad (9)$$

The error signal is fed to the PI controller, which yields estimated rotor resistance.

4. 2. MRAS Based Rotor Resistance Estimation Using Reactive Power

In Maiti et al.'s paper [17], the MRAS-RP (Figure 7), the reference model and adjustable model compute instantaneous reactive power (Q_{ref}) and steady state reactive power (Q_{est}) respectively.
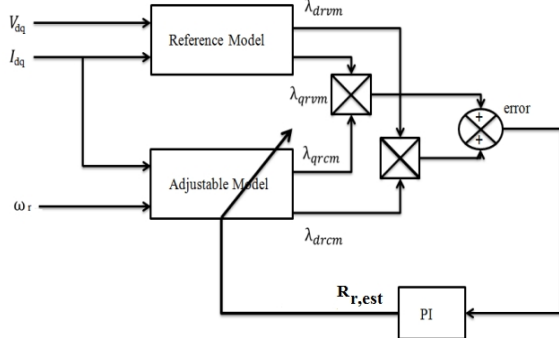

Figure 6. Rotor Flux based MRAS for Rotor Resistance Estimation

Note that the reference model is independent of slip speed (ω_{sl}) whereas the adjustable model depends on ω_{sl}. The error signal ($\varepsilon = Q_{ref} - Q_{est}$) is fed to the adaptation mechanism block (adaptation mechanism is done using PI-controller), which yields estimated slip speed ($\omega_{sl,est}$). The rotor resistance (R_r) is then calculated from $\omega_{s,est}$.

$$V_{ds} = R_s i_{ds} + \sigma L_s \frac{d}{dt} i_{ds} + \frac{L_m}{L_r} \frac{d}{dt} \psi_{dr} - \sigma L_s \omega_e i_{qs} - \omega_e \frac{L_m}{L_r} \psi_{qr} \quad (10)$$

$$V_{qs} = R_s i_{qs} + \sigma L_s \frac{d}{dt} i_{qs} + \frac{L_m}{L_r} \frac{d}{dt} \psi_{qr} + \sigma L_s \omega_e i_{ds} + \omega_e \frac{L_m}{L_r} \psi_{dr} \quad (11)$$

Where, $\omega_e = \omega_r + \omega_{sl}$

The instantaneous reactive power is given as:

$$Q_{ref} = V_{qs} i_{ds} - V_{ds} i_{qs} \quad (12)$$

It is worthwhile to mention that the above expressions of Q are free from stator resistance, which is a notable feature of any reactive power-based scheme. In steady state the derivative terms are zero. Substituting Equations (10) and (11) in Equation (12):

$$Q_{est} = \omega_e \sigma L_s (i_{ds}^2 + i_{qs}^2) + \omega_e \frac{L_m}{L_r} (\psi_{qr} i_{qs} + \psi_{dr} i_{ds}) \quad (13)$$

Substituting the condition $\psi_{dr} = L_m i_{ds}$ and $\psi_{qr} = 0$ for the indirect field-oriented control Induction Motor drive in Equation (11), the more simplified expression of Q is:

$$Q_{est} = \omega_e \sigma L_s (i_{ds}^2 + i_{qs}^2) + \omega_e \frac{L_m^2}{L_r} i_{ds}^2 \quad (14)$$

From the above expressions of Q_{ref} is chosen as the reference model as it does not comprise any slip-speed term. Q_{est} may be used in the adjustable model. Moreover, Q_{est} is dependent on slip speed.
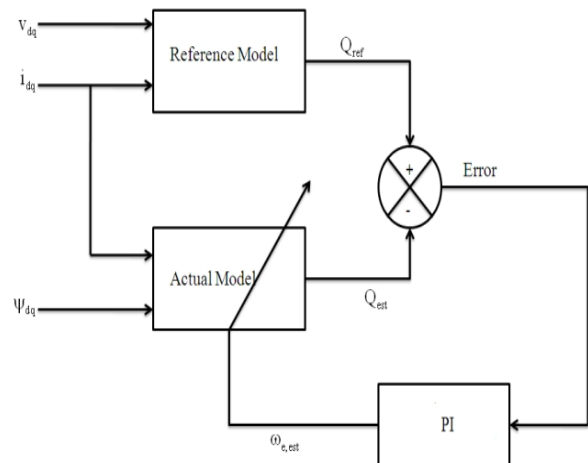

Figure 7. Reactive Power based MRAS for Rotor Resistance Estimation

5. SIMULATION RESULTS

In order to verify the effectiveness and feasibility of estimating rotor resistance using MRAS-Rotor Flux method and MRAS-Reactive Power method, a simulation model has been developed in MATLAB/SIMULINK platform. The space vector PWM based vector controlled drive is subjected to changes in rotor resistance and the tracking capability of both MRAS-RF and MRAS-RP method are compared. Simulations have been done for various changes in R_r for the operating condition of 415V/50Hz and rated load of 7.5Nm and the performance of Rotor Resistance Estimator has been analysed.

1. 100% step change in R_r
2. 100% trapezoidal change in R_r

Figure 8 shows the performance of RF-MRAS and RP-MRAS for step change in rotor resistance. The rotor resistance of 6.085 is step change to 12.17 (100% change in R_r) at 1sec. From the obtained results, it is observed that the R_r estimated from the RP-MRAS closely tracks the actual with lesser error and settles faster with the actual as compared to R_r estimated from the RF-MRAS. It is also noted that the ripple content is more in the R_r estimated from the RF-MRAS whereas in RP-MRAS method ripple content in the estimated R_r is found to be less.

Figure 9 shows the performance of both the MRAS schemes for trapezoidal change in R_r. The R_r gradually increases from 0.4sec to 0.8sec and reaches the value from 6.085 to 12.17 (100% change in R_r). From 0.8sec to 1.4sec, the value is maintained at 12.17. From 1.4sec to 1.8sec, R_r decreases gradually and reaches again to 6.085. In this case, R_r also estimated from the RP-MRAS which is having less ripple whereas ripple content is more in the R_r estimated from the RF-MRAS. Thus, for all the changes (step and trapezoidal change) the performance of RP-MRAS is superior as compared to RF-MRAS. The steady state error and settling time for both the MRAS schemes for various changes in R_r are consolidated and presented in Tables 2 and 4, respectively.

The Tables 2 and 4 show that the error between actual rotor resistance and estimated rotor resistance and settling time for various changes in rotor resistance using MRAS-RF and MRAS-RP methods and Table 3 and 5 shows the performance of MRAS-RF and MRAS-RP based rotor resistance estimator for various voltages with rated load condition. From the obtained results, it is observed that the error between the actual and estimated R_r is always within 1.1% for MRAS-RP method and 3% for MRAS- RF method. Settling time is found to be approximately 0.05sec for MRAS-RP method and 0.1sec for MRAS-RF method.
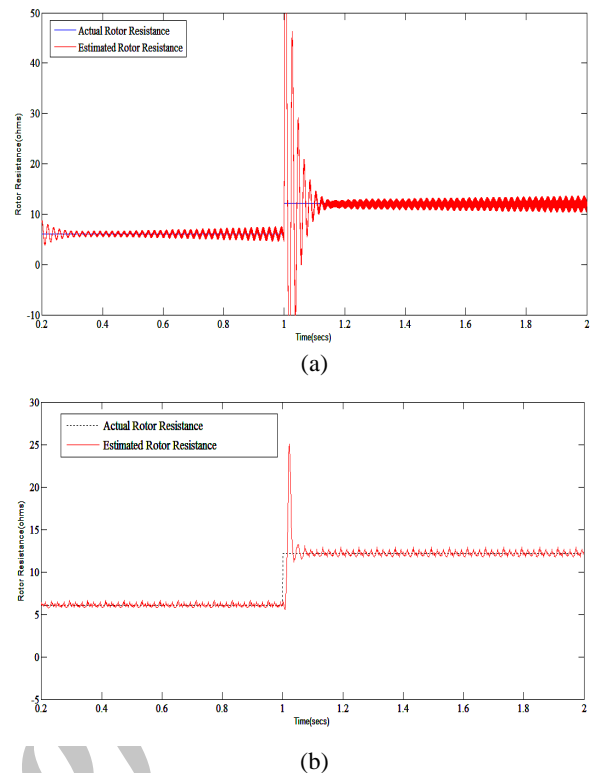

(a)

(b)

Figure 8. Actual and Estimated Rotor Resistance for 100% step change a) RF – MRAS b) RP-MRAS
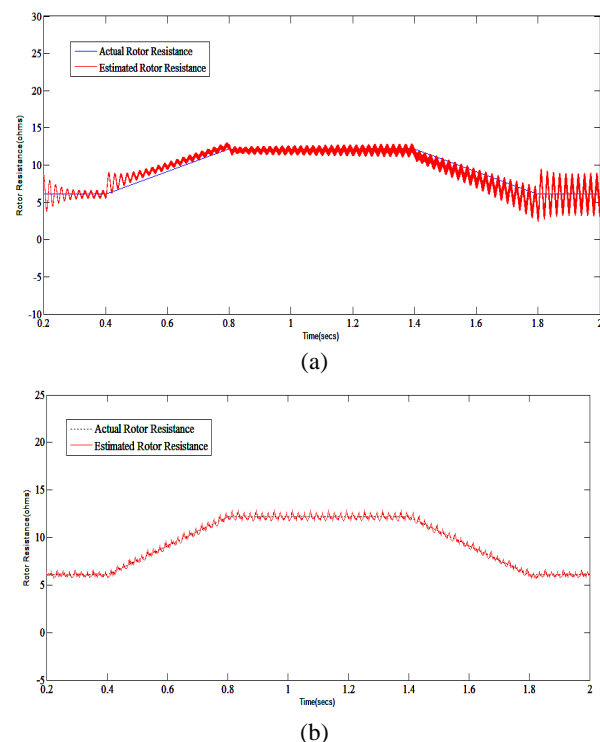

(a)

(b)

Figure 9. Actual and Estimated Rotor Resistance for 100% Trapezoidal change. a) RF – MRAS b) RP-MRAS

TABLE 2. Estimator error and settling time for various change in rotor resistance using MRAS – Rotor Flux (RF-MRAS) Method

Change in R_r (%)	Actual R_r(ohms)	Estimated R_r(ohms)	Settling Time(sec)	Error (%)
10	6.694	6.91	0.1	3.125
20	7.302	7.515	0.1	2.834
30	7.910	8.124	0.1	2.634
40	8.519	8.734	0.1	2.461
50	9.127	9.341	0.1	2.290
60	9.736	9.943	0.1	2.081
70	10.34	10.54	0.1	1.897
80	10.95	11.14	0.1	1.705
90	11.56	11.73	0.1	1.449
100	12.17	12.31	0.1	1.137

TABLE 3. MRAS-RF based rotor resistance estimation for various voltages with rated load

S.no.	Voltage (V)	Actual $R_r$ohms	Estimated $R_r$ohms	Error (%)	Settling Time (sec)
1	415	10.95	11.14	1.705	0.1
2	300	10.95	11.14	1.705	0.1
3	200	10.95	11.14	1.705	0.1
4	100	10.95	11.14	1.705	0.1
5	10	10.95	11.14	1.705	0.1

TABLE 4. Estimator error and settling time for various change in rotor resistance using MRAS – Reactive Power (RP-MRAS) Method

Change in R_r (%)	Actual R_r(ohms)	Estimated R_r(ohms)	Settling Time(sec)	Error (%)
10	6.694	6.774	0.05	1.181
20	7.302	7.386	0.05	1.137
30	7.910	7.998	0.04	1.100
40	8.519	8.609	0.04	1.045
50	9.127	9.221	0.04	1.019
60	9.736	9.833	0.03	0.986
70	10.34	10.44	0.03	0.957
80	10.95	11.06	0.03	0.995
90	11.56	11.67	0.03	0.943
100	12.17	12.28	0.03	0.896

TABLE 6. Comparison of estimator error and settling time between MRAS-RF and MRAS-RP methods

Methods	Error (%)	Settling Time (sec)
MRAS - RF	3	0.1
MRAS - RP	1.1	0.05

TABLE 5. MRAS-RP based rotor resistance estimation for various voltages with rated load

S.no.	Voltage (V)	Actual Rrohms	Estimated Rrohms	Error (%)	Settling Time (sec)
1	415	10.95	11.06	0.995	0.03
2	300	10.95	11.06	0.995	0.03
3	200	10.95	11.06	0.995	0.03
4	100	10.95	11.06	0.995	0.03
5	10	10.95	11.06	0.995	0.03

The maximum estimation error and maximum settling time for MRAS-RP and MRAS-RF based rotor resistance estimator is discussed in Table 6. From Table 6, it is observed that the estimation error and settling time of MRAS-RP method is found to be less compared to MRAS-RF based method.

6. CONCLUSION

The performance of Vector Controlled Induction Motor (IM) Drive to a large extent depends on the accuracy of rotor resistance estimation. In this paper, MRAS based rotor resistance estimator using Flux and reactive power techniques is studied, designed and validated through MATLAB simulation. Their performance is analyzed extensively for various changes in rotor resistance and compared in terms of accuracy and settling time. The maximum percentage error of RP-MRAS is lesser than the RF-MRAS method. The R_r estimated from the RP-MRAS is having less ripple whereas the ripple content is more in the R_r estimated from the RF-MRAS. Selection of reactive power as a state variable in MRAS technique makes the system simpler and easier to design. Thus, RP-MRAS is identified to be superior in terms of accuracy and settling time, as compared to RF-MRAS and found to be promising for rotor resistance estimation for Space Vector PWM Inverter fed Induction Motor drives. The ripple content presented in the R_r can be reduced using Neural Learning Based MRAS and can be considered as future scope of this work.

7. REFERENCES

1. Mohan, N., Undeland, T. and Robbins, W., "Power Electronics: Converters, Applications and Design", 2en ed., New York, Wiley, 1995.

2. Krishnan, R. and Bharadwaj, S., "A Review of Parameter Sensitivity and Adaptation in Indirect Vector Controlled Induction Motor Drive System", *IEEE Transactions on Power Electronics*, Vol. 6, No. 4, (1991).

3. Murphy, J.M.D. and Turnbull, F.G., "Power Electronics Control of A.C .Motors" Oxford: Pergamon Press, (1988).

4. Blaschke, F., "The principle of field orientation as applied to the new transvector closed loop system for rotating field machines", *Siemens Review*, Vol. 34, (1972), 217-220.

5. Bimal, K.B., "Modern power electronics and ac drives", Pearson Education, India, (2003).

6. Vas, P., "Vector Control of AC Machines", Oxford Science Publications, (1990).

7. Krishnan, R. and Doran, F.C., "Study of parameter sensitivity in high performance inverter-fed induction motor drive systems", *IEEE Transactions on Industry Applications*, Vol, IA-23, No. 4, (1987), 623-635.

8. Karanayil, M., Rahman M.F. and Grantham, C., "Online Stator and Rotor Resistance Estimation Scheme Using Artificial Neural Networks for Vector Controlled Speed Sensorless Induction Motor Drive" *IEEE Transactions on Industrial Electronics*, Vol. 54, No. 1, (2007).

9. Mondal, S.K., Pinto, J.O.P. and Bose, B.K., "A neural network based space vector PWM controller for a three voltage fed inviter induction motor drive," *IEEE Transaction on Industry Application,* Vol. 30, No. 3, (2002), 660-669.

10. Nomura, M., Ashikaga, T., Terashima, M. and Nakamura, T., "A high response induction motor control system with compensation for secondary resistance variation", in *Proc. IEEE PESC,* (1987), 46-51.

11. Wade, S., Dunnigan, M.W. and Williams, B.W., "A new method of rotor resistance estimation for vector controlled induction machines", *IEEE Transaction on Industry Electronics*, Vol. 44, No. 2, (1997), 247-257.

12. Karanayil, B., Rahman, M.F. and Grantham, C., "On-line stator and rotor resistance estimation scheme using artificial neural networks for vector controlled speed sensor less induction motor drive", *IEEE Transaction on Industry Electronics*, Vol. 54, No. 1, (2007), 167-176.

13. Garces, L., "Parameter adaptation for the speed controlled static ac drive with a squirrel-cage Induction motor", *IEEE Transaction on Industry Application,* Vol. IA-16, No. 2, (1980), 173-178.

14. Nait Said, M.S. and Benbouzid, M.E.H., "Induction motors direct field oriented control with robust on-line tuning of rotor resistance", *IEEE Transaction on Energy conversion,* Vol. 14, No. 4, (1999), 1038-1042.

15. Stephan, J., Bodson, M. and Chiasson, J., "Real-time estimation of induction motor parameters," *IEEE Transaction on Industry Application,* Vol. 30, No. 3, (1994), 746–759.

16. Bin, H., Wenlong, Q. and Haifeng, L., "A novel on-line rotor resistance estimation method for vector controlled induction motor drive" *in Proc. Conf. Rec. IEEE IPEMC Conf.*, Vol. 2, (2004), 655-660.

17. Maiti, S., Chakraborty, Ch., Hori Y. and Minh, C. T., "Model Reference Adaptive Controller-based Rotor Resistance and Speed Estimation Techniques for Vector Controlled Induction Motor Drive Utilizing Reactive Power*", IEEE Transactions on Industrial Electronics*, Vol. 55, No. 2, (2008).

18. Hadj Said, S., Mimouni, M.F., Sahli F.M. and Farza, M., "High gain observer based on-line rotor and stator resistances estimation for IMs", *Simulation Modelling Practice and theory*, Vol. 19, No. 7, (2011), 1518-1529.

19. Godpromesse, k., Tarek, A.-A., Francoise, L.– L., Amir, A. and Jean Claude, V., "An improved rotor resistance estimator for Induction Motors adaptive control", Electrical Power Systems Research, (2011).

20. Kenne, G., Simo, R.S., Lamnabhi, L.F., Arzande, A. and Vannier, J.C., "An on-line simplified rotor resistance estimator for induction motors", *IEEE Transactions on Control Systems Technology,* Vol. 18, No. 5, (2010), 1188-1194.

21. Karanayil, M., Rahman, M.F. and Grantham, C., "Identification of Induction Motor Parameters in Industrial Drives with Artificial Neural Networks", Research Article, in *Advances in Fuzzy Systems Hindawi Publishing Corporation*, (2009).

22. Gupta, A.K. and Khambadkone, A.M., "A general space vector PWM algorithm for multilevel inverters, including operation in over modulation range", *IEEE Transactions on Power Electronics,* Vol. 22, No. 2, (2007), 517-526.

23. Zhou, K. and Wang, D., "Relationship between Space – Vector Modulation and Three-Phase Carrier-Based PWM: A Comprehensive Analysis", *IEEE Transactions on Industrial Electronics,* Vol. 49, No. 1, (2002).

APPENDIX

INDUCTION MOTOR RATINGS

Parameters	Values
Rated Power:	1.1 KW
Rated voltage:	415V
Rated current:	2.7A
Type:	3 Phase
Frequency:	50Hz
Number of poles:	4
Stator Resistance (R_s):	6.03Ω
Rotor Resistance (R_r):	6.085Ω
Magnetizing Inductance (L_m):	0.4893H
Stator Inductance (L_s):	0.5192H
Rotor Inductance (L_r):	0.5192H
Inertia J_{tot}:	0.01178Kgm^2
Friction B:	0.0027Kgm^2/s
Rated Torque:	7.5Nm

Comparison of MRAS Based Rotor Resistance Estimator Using Reactive Power and Flux Based Techniques for Space Vector PWM Inverter Fed Induction Motor Drives

M. Nandhini Gayathri [a,] S. Himavathi [b], R. Sankaran[a]

[a] Department of EEE, SASTRA University, Thanjavur -613 402, India
[b] Department of EEE, Pondicherry Engineering College, Puducherry - 605014, India

---

چکیده

عملکرد حامل کنترل کننده موتور القایی سواری وابسته به دقیق بودن مقاومت روتاری (قسمت چرخان موتور) است که ان نیز (مقاومت روتاری) با تغییرات دما و بسامد تغییر خواهد کرد. MRAS با استفاده از نیروی واکنش و شار (flux) به عنوان یک حالت متغییر برای تخمین مقاومت روتاری بهدست می‌اید (استفاده از این روش) که محاسبه MARS را اسان‌تر نموده و طراحی را ساده‌تر می‌کند. در این مقاله، شار روتاری بر اساس MRAS (RF-MRAS) و نیروی واکنش بر اساس MRAS (RP-MRAS) برای تخمین مقاومت روتاری طراحی شده است و اعتبار ان با استفاده از نرم‌افزار مطلب شبیه‌سازی شده است. عملکرد این دو روش به دقت بررسی شده و از نظر دقت و زمان ته‌نشینی انها با هم مقایسه شده است. روش مناسب برای تخمین مقاومت روتاری برای حامل فضایی PWM معکوس کننده موتورسواری القایی نیز تعیین شده است و نتایج بهدست امده ارائه شده است.

doi: *10.5829/idosi.ije.2012.25.03c.04*